AMERICAN SOCIETY FOR MICROBIOLOGY | Applied and Environmental Microbiology®

ENZYMOLOGY AND PROTEIN ENGINEERING

Mutant Variants of the Substrate-Binding Protein DppA from *Escherichia coli* Enhance Growth on Nonstandard γ-Glutamyl Amide-Containing Peptides

Tilmann Kuenzl,[a] Xiaochun Li-Blatter,[b] Puneet Srivastava,[c] Piet Herdewijn,[c] Timothy Sharpe,[b] Sven Panke[a]

[a]Bioprocess Laboratory, Department of Biosystems Science and Engineering, ETH Zurich, Basel, Switzerland
[b]Biophysics Facility, Biozentrum, University of Basel, Basel, Switzerland
[c]Laboratory of Medicinal Chemistry, Rega Institute for Medical Research, KU Leuven, Leuven, Belgium

ABSTRACT The import of nonnatural molecules is a recurring problem in fundamental and applied aspects of microbiology. The dipeptide permease (Dpp) of *Escherichia coli* is an ABC-type multicomponent transporter system located in the cytoplasmic membrane, which is capable of transporting a wide range of di- and tripeptides with structurally and chemically diverse amino acid side chains into the cell. Given this low degree of specificity, Dpp was previously used as an entry gate to deliver natural and nonnatural cargo molecules into the cell by attaching them to amino acid side chains of peptides, in particular, the γ-carboxyl group of glutamate residues. However, the binding affinity of the substrate-binding protein dipeptide permease A (DppA), which is responsible for the initial binding of peptides in the periplasmic space, is significantly higher for peptides consisting of standard amino acids than for peptides containing side-chain modifications. Here, we used adaptive laboratory evolution to identify strains that utilize dipeptides containing γ-substituted glutamate residues more efficiently and linked this phenotype to different mutations in DppA. *In vitro* characterization of these mutants by thermal denaturation midpoint shift assays and isothermal titration calorimetry revealed significantly higher binding affinities of these variants toward peptides containing γ-glutamyl amides, presumably resulting in improved uptake and therefore faster growth in media supplemented with these nonstandard peptides.

IMPORTANCE Fundamental and synthetic biology frequently suffer from insufficient delivery of unnatural building blocks or substrates for metabolic pathways into bacterial cells. The use of peptide-based transport vectors represents an established strategy to enable the uptake of such molecules as a cargo. We expand the scope of peptide-based uptake and characterize in detail the obtained DppA mutant variants. Furthermore, we highlight the potential of adaptive laboratory evolution to identify beneficial insertion mutations that are unlikely to be identified with existing directed evolution strategies.

KEYWORDS peptide transport, portage transport, γ-glutamyl transferase, membrane transport, isothermal titration calorimetry, adaptive laboratory evolution, substrate specificity, ABC transporters, synthetic biology, dipeptide permease, gamma-glutamyl transferase

Transport across membranes is an often-undervalued factor that frequently limits metabolic engineering or synthetic biology approaches due to insufficient uptake of potentially interesting molecules (1). Several approaches to develop broadly applicable solutions to overcome limitations in membrane transport have been presented

Received 8 February 2018 **Accepted** 26 April 2018

Accepted manuscript posted online 4 May 2018

Citation Kuenzl T, Li-Blatter X, Srivastava P, Herdewijn P, Sharpe T, Panke S. 2018. Mutant variants of the substrate-binding protein DppA from *Escherichia coli* enhance growth on nonstandard γ-glutamyl amide-containing peptides. Appl Environ Microbiol 84:e00340-18. https://doi.org/10.1128/AEM.00340-18.

Editor Claire Vieille, Michigan State University

Address correspondence to Sven Panke, sven.panke@bsse.ethz.ch.

during the last decades, most of them using peptides as transport vectors and taking advantage of the low substrate specificity of peptide transporters. It was previously reported that cargo molecules can be delivered into the cell by attaching them to the N or C termini or specific amino acid side chains of di- or tripeptides, from where they would eventually be released inside the cell by endogenous peptidases or chemical decomposition of the transport vector-cargo construct (2–8). We recently presented a synthetic transport system that enables the uptake of cargo molecules into *Escherichia coli* by attaching them via a stable amide linkage to the γ-carboxyl group of a glutamate residue of the dipeptide alanyl-glutamate (Ala-Glu) (9). Once the peptide harboring the γ-glutamyl amide has been taken up, the N-terminal alanine residue is removed by intracellular peptidases, and the liberated γ-glutamyl amide is further hydrolyzed by a cytoplasmic variant of the enzyme γ-glutamyl transferase from *Pseudomonas nitroreducens* (*Pn*GGT) to release the cargo molecule inside the cell. With this system, we were able to demonstrate the uptake of different natural and nonnatural cargo molecules, offering a more general and potentially versatile approach to overcome transport problems in *E. coli*.

Clearly, the versatility of the system depends largely on the substrate specificity of the bacterial peptide importers, which belong to the class of ATP-binding cassette (ABC) transporters. ABC transporters are multisubunit transporters that play a fundamental role in regulation of the uptake of nutrients into and the secretion of toxic or harmful compounds out of the cell (10). Most of them evolved to be highly specialized for the transport of a single compound or small groups of structurally similar compounds across membranes. Corresponding to this high degree of specificity, bacteria have developed a broad spectrum of ABC transporters to deal with the import of a broad range of different compounds (11). In *E. coli*, ABC transporters are the largest paralogous protein family, with their genes occupying approximately 5% of the *E. coli* genome (12). ABC transporters are usually composed of two transmembrane proteins that form a membrane channel and two nucleotide-binding proteins that generate energy for the translocation process by hydrolyzing ATP on the cytoplasmic side of the membrane. Additionally, ABC transporters often have soluble substrate-binding proteins (SBPs) that capture their substrates in the periplasmic space of Gram-negative or the extracellular space of Gram-positive bacteria and deliver them to their respective transmembrane proteins.

The *E. coli* peptide transporters dipeptide permease (DppABCDF) and oligopeptide permease (OppABCDF) are the main uptake routes for peptides from the environment and are known to have rather relaxed substrate specificities (13). Dipeptide permease has a preference for dipeptides and only little affinity for certain tripeptides (14, 15). Oligopeptide permease, on the other hand, prefers tripeptides but can transport larger peptides up to hexapeptides with reduced efficiency (16–18). To be transported by the dipeptide or oligopeptide permease transport systems, peptides have to be captured in the periplasmic space by the non-membrane-attached SBPs DppA or OppA, which, to a large extent, determine the substrate specificities of their transporters (19, 20). Both SBPs possess large water-filled binding pockets that can accommodate peptides with structurally diverse amino acid side chains, thereby contributing to the low substrate specificity of the two transporters (21, 22). Despite this rather low degree of specificity, it was demonstrated that DppA is less tolerant toward peptides with side-chain modifications than OppA (23).

In this study, we aimed to investigate the uptake of peptides containing γ-substituted glutamate residues in more detail in view of possible expansions of the uptake spectrum, using an experimental system for which we assume that the uptake of suitable substrates is the limiting factor in the complementation of growth auxotrophies. Mutations in the periplasmic SBP DppA that led to improved utilization of these peptides were identified by adaptive laboratory evolution. Characterization of the DppA variants by thermal denaturation midpoint shift assays and isothermal titration calorimetry (ITC) confirmed that the mutations had indeed increased the binding affinity toward peptides containing γ-glutamyl amides. The results obtained in

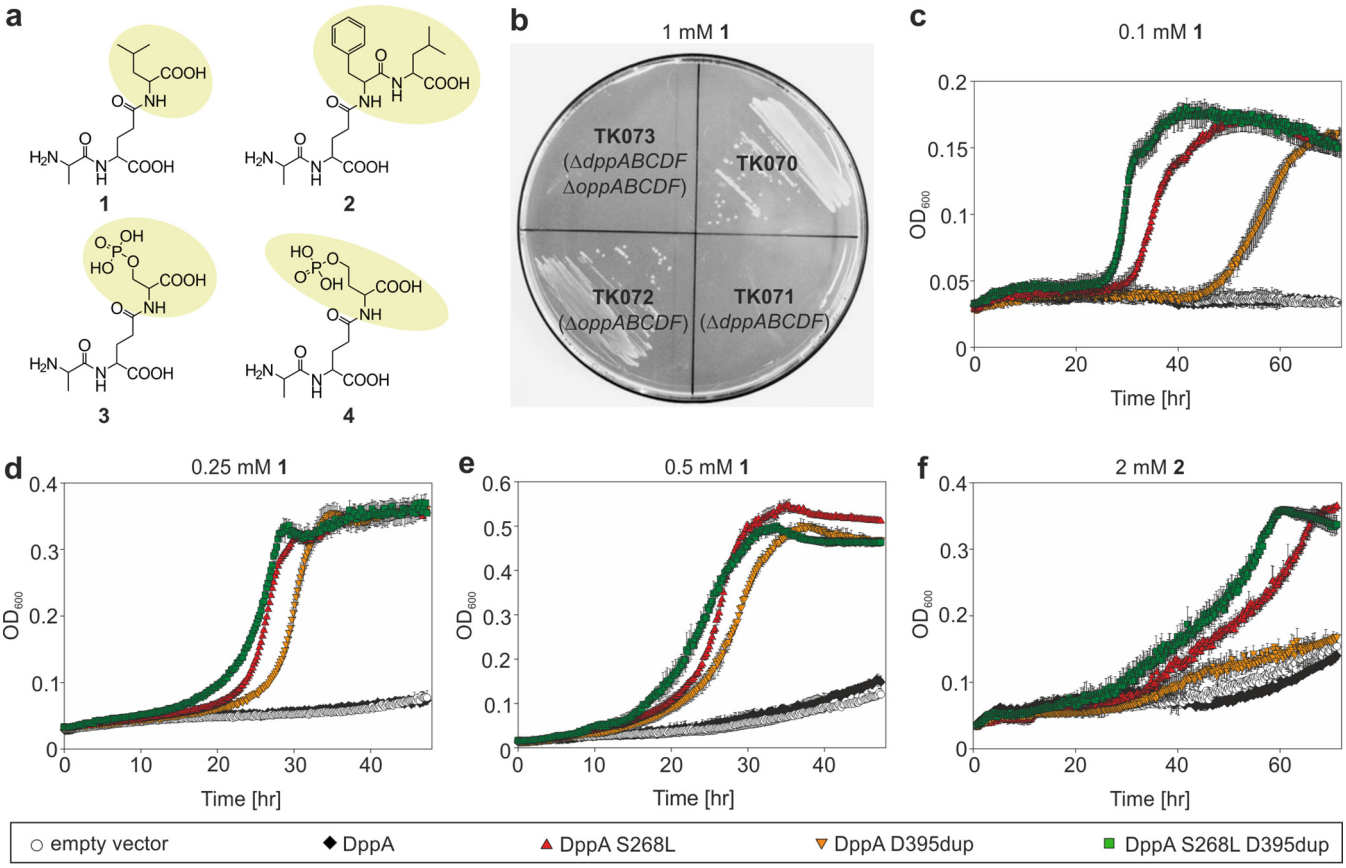

FIG 1 Uptake of dipeptides containing γ-substituted glutamates. (a) The following peptides were used in this study: Ala-γ-Glu-Leu (1), Ala-γ-Glu-Phe-Leu (2), Ala-γ-Glu-*O*-phospho-L-serine (SEP) (3), and Ala-γ-Glu-*O*-phospho-L-homoserine (PHS) (4). The respective cargoes of the peptides are highlighted in yellow. (b) The leucine auxotrophic selection strains TK070, TK071, TK072, and TK073 were transformed with p*Pn*GGT and reisolated on plates containing M9 minimal medium supplemented with 0.5% glucose, 0.5 mM IPTG, and 1 mM Ala-γ-Glu-Leu. The plate was incubated for 2 days at 37°C. (c) Strain TK070/p*Pn*GGT was transformed with the plasmids pSEVA271 (empty vector), pSEVA271/*dppA* (synthesizing DppA), pSEVA271/*dppA*_S268L (DppA S268L), pSEVA271/*dppA*_D395dup (DppA D395dup), and pSEVA271/*dppA*_S268L_D395dup (DppA S268L D395dup). (c to e) Growth was tested in liquid M9 minimal medium supplemented with 0.5% glucose, 0.5 mM IPTG, 100 ng · ml^{-1} anhydrotetracycline, and 0.1 mM (c), 0.25 mM (d), or 0.5 mM (e) the peptide Ala-γ-Glu-Leu. (f) Similar growth experiment in liquid M9 minimal medium supplemented with 0.5% glucose, 0.5 mM IPTG, 100 ng · ml^{-1} anhydrotetracycline, and 2 mM the peptide Ala-γ-Glu-Phe-Leu. Error bars in the growth curves represent the standard deviation from 3 replicates.

this study constitute a significant improvement in our previously described synthetic transport system.

RESULTS

Identification of transporters involved in Ala-γ-Glu-Leu uptake. We previously reported that the peptide Ala-γ-Glu-Leu (Fig. 1a, peptide 1), an Ala-Glu dipeptide with a leucine attached to the γ-carboxyl group of Glu, can be taken up by *E. coli* and used as sole source of leucine, provided that the leucine residue is released intracellularly from the glutamate side chain by a cytoplasmic variant of the enzyme *Pn*GGT (9). To analyze the uptake of Ala-γ-Glu-Leu in more detail, we aimed to identify the uptake route of this peptide. For this, the *dppABCDF* and *oppABCDF* operons, encoding the versatile dipeptide and oligopeptide permease transport systems, respectively, were deleted in the leucine auxotrophic selection strain TK070 (see Table 4), resulting in strains TK071 (Δ*dppABCDF*), TK072 (Δ*oppABCDF*), and TK073 (Δ*dppABCDF* Δ*oppABCDF*). All strains were transformed with plasmid p*Pn*GGT to synthesize the cytoplasmic *Pn*GGT variant, and the resulting strains were tested for growth on plates containing M9 minimal medium supplemented with glucose and the peptide Ala-γ-Glu-Leu (1 mM) as the sole source of leucine (Fig. 1b). Only the two strains carrying a deletion in the *dppABCDF* operon were unable to grow on this medium, indicating that the peptide Ala-γ-Glu-Leu is exclusively taken up via the Dpp dipeptide permease transport system.

Adaptive laboratory evolution to improve utilization of Ala-γ-Glu-Leu. The growth of strain TK070/p*Pn*GGT was restored in minimal medium supplemented with glucose and 1 mM Ala-γ-Glu-Leu but was hardly detectable if peptide concentrations were lower than 0.5 mM. These concentrations are relatively high compared to the concentrations of free leucine or leucine-containing peptides that are required at approximately 0.1 to 0.4 mM to restore growth of a leucine auxotrophic *E. coli* strain (24), which indicates inefficiencies in uptake or intracellular processing of Ala-γ-Glu-Leu. To improve growth at low concentrations of this peptide, adaptive laboratory evolution experiments were performed. Adaptive laboratory evolution is a method to accumulate evolutionary changes in microbial populations during long-term selection under specified growth conditions (25). For this, leucine auxotrophic strain TK070 was freshly transformed with p*Pn*GGT and plated on a plate containing M9 minimal medium supplemented with 0.5% glucose, 0.5 mM isopropyl-β-D-thiogalactopyranoside (IPTG), and only 0.1 mM Ala-γ-Glu-Leu. After a 10-day incubation period at 37°C, the formation of small colonies was detected, and the adaptive phenotype was verified by reisolating these colonies on plates containing the same medium (Fig. S1). In total, three of the isolated strains grew significantly faster than the parent strain at low peptide concentrations.

To identify possible reasons for the improved growth of the isolated strains, genomic DNA was prepared and analyzed by next-generation sequencing. A comparison of the genomic sequences of the mutant and the parent strains revealed that all three mutant strains had acquired mutations in the gene *dppA*, encoding the periplasmic binding protein of dipeptide permease, which had been shown to be responsible for the uptake of Ala-γ-Glu-Leu. One strain had a point mutation at amino acid position 268, causing an amino acid change from serine to leucine (DppA S268L). The other two strains had duplications of residues D395 (DppA D395dup) and T418 (DppA T418dup), respectively. No additional mutations were identified in these strains or the p*Pn*GGT plasmids isolated from these strains.

***In vivo* characterization of DppA variants.** To further investigate the impact of the adaptive *dppA* mutations, a wild-type *dppA* gene was cloned into the low-copy-number vector pSEVA271 under the control of a tetracycline-inducible promoter, resulting in plasmid pSEVA271/*dppA*, and the identified *dppA* mutations were introduced by site-directed mutagenesis. The influence of *dppA* overexpression was analyzed in strain TK070/p*Pn*GGT additionally transformed with the *dppA* expression plasmids, and growth was tested in liquid M9 minimal medium supplemented with glucose and with various concentrations of the peptide Ala-γ-Glu-Leu. At 0.1 mM Ala-γ-Glu-Leu, no growth was detected if the strain was transformed with the empty vector pSEVA271 or plasmid pSEVA271/*dppA* containing the *dppA* wild-type gene (Fig. 1c; also see Table S1 in the supplemental material). If, however, wild-type DppA was replaced by the S268L or D395dup mutant variant, growth was observed at this peptide concentration. The fastest growth was observed when the S268L D395dup double mutant was synthesized, indicating a combinatorial effect of the two mutations in *dppA*. Similar results were obtained at a concentration of 0.25 mM Ala-γ-Glu-Leu. Here, all strains that synthesized DppA mutant variants were able to grow, and no significant differences between these strains were observed (Fig. 1d and Table S1). At 0.5 mM Ala-γ-Glu-Leu, all strains synthesizing the DppA mutant variants grew rapidly, while only residual growth was detected if the strain was transformed with the empty vector pSEVA271 or plasmid pSEVA271/*dppA* (Fig. 1e and Table S1). This residual growth was presumably observed because of the continuing presence of the endogenous dipeptide permease components that were still encoded on the chromosome of strain TK070. Initially, we attempted to perform growth experiments in *dppA* or *dppABCDF* deletion strains. However, deleting *dppA* turned out to lead to polar effects on other genes of the *dpp* operon. Deleting the entire *dpp* operon and expressing all transporter components from a plasmid, on the other hand, led to a severe reduction in cell viability. Therefore, we chose the strategy in which we overexpress only *dppA* from a plasmid and thereby

TABLE 1 Kinetic measurements with purified *Pn*GGT and the substrates γ-Glu-Leu and γ-Glu-Phe-Leu

Measurement	γ-Glu-Leu	γ-Glu-Phe-Leu
K_m (μM) (mean ± SD)[a]	145.1 ± 27.6	1,335 ± 303
V_{max} (mean ± SD) (μmol · min^{-1} · mg^{-1})[a,b]	24.7 ± 1.39	8.41 ± 0.765
k_{cat} (s^{-1})[c]	24.4	8.31
k_{cat}/K_m (mM^{-1} · s^{-1})	168	6.22

[a]Calculated from triplicate measurements.
[b]The reaction curves are shown in Fig. S3.
[c]Values were calculated from the mean values for V_{max}.

outcompete the endogenous DppA variant. The significant differences in growth between strains synthesizing wild-type DppA and DppA mutant variants indicate that this strategy was valid. Improved growth at low peptide concentrations was also observed when synthesizing DppA T418dup, but this mutant was not further analyzed due to its detrimental effect on protein stability (see below). Taken together, these data indicate that the mutations identified in *dppA* led to improved uptake of Ala-γ-Glu-Leu at low peptide concentrations. Similar experiments in strain TK071 (Δ*dppABCDF*) confirmed that the beneficial effects of the DppA mutant variants only occur if all components of the dipeptide permease are present (Fig. S2).

The results obtained until this point raised the question if the identified *dppA* mutations specifically improved utilization of the peptide Ala-γ-Glu-Leu or if peptides containing other cargo molecules attached to the glutamate side chain would be affected as well, which would greatly contribute to the generality of the synthetic transport system. To investigate this, similar growth assays were performed with the peptide Ala-γ-Glu-Phe-Leu (Fig. 1a, peptide 2). Due to the additional phenylalanine residue attached to the glutamate side chain, the cargo load of this peptide differs considerably in size and structure from the cargo load of the peptide Ala-γ-Glu-Leu, but it still offers the possibility to select for growth with a leucine auxotrophic selection strain. Therefore, strain TK070 harboring p*Pn*GGT and the same derivatives of pSEVA271/*dppA* was grown in liquid M9 minimal medium supplemented with 2 mM Ala-γ-Glu-Phe-Leu, and results were obtained comparable to those with Ala-γ-Glu-Leu (Fig. 1f and Table S1). Strains synthesizing the DppA mutant variants S268L and S268L D395dup grew significantly faster in this medium than strains carrying an empty vector or synthesizing wild-type DppA, while the strain synthesizing the DppA D395dup mutant variant grew only slightly faster than the controls. However, it has to be noted that the required concentration of Ala-γ-Glu-Phe-Leu in the growth medium was higher than that in the experiments with Ala-γ-Glu-Leu. The two most likely explanations for this increased demand for Ala-γ-Glu-Phe-Leu were either reduced transport of the peptide into the cell or inefficient hydrolysis of the intracellular cleavage product γ-Glu-Phe-Leu by *Pn*GGT.

To analyze the hydrolysis of this cleavage product by *Pn*GGT, the kinetic parameters of *Pn*GGT were determined with the substrates γ-Glu-Leu and γ-Glu-Phe-Leu. The measurements revealed that *Pn*GGT has a 9.2-fold lower K_m for γ-Glu-Leu than for γ-Glu-Phe-Leu and a 3-fold higher V_{max} for γ-Glu-Leu than for γ-Glu-Phe-Leu, resulting in an approximately 27-fold higher catalytic efficiency (k_{cat}/K_m) of *Pn*GGT for γ-Glu-Leu (Table 1 and Fig. S3a and b). These findings indicate that slower growth on Ala-γ-Glu-Phe-Leu can be explained at least in part by less efficient enzymatic release of the cargo Phe-Leu by *Pn*GGT. At the same time, the mutations identified in *dppA* seem to improve growth on peptides containing cargo molecules that vary markedly in size and structure, suggesting that these findings can potentially be transferred to future applications of the transport system.

Synthesis and purification of DppA mutant variants. Faster utilization of peptides containing γ-glutamyl amides by strains synthesizing DppA mutant variants can potentially be explained by improved affinity of the DppA mutant variants for these peptides. Improved binding might lead to enhanced delivery of peptides to the

TABLE 2 Thermal shift assays with DppA wild type and mutants[a]

DppA wild type or mutant	T_m (°C), unbound	ΔT_m (°C), Ala-γ-Glu-Leu	ΔT_m (°C), Ala-γ-Glu-Phe-Leu
DppA	70.5 ± 0.1	2.4 ± 0.1	2.0 ± 0.1
D395dup	62.0 ± 0.1	3.1 ± 0.1	2.8 ± 0.1
S268L	60.5 ± 0.1	3.3 ± 0.2	4.7 ± 0.2
T418dup	50.0 ± 0.2	4.5 ± 0.2	6.7 ± 0.2
S268L D395dup	54.4 ± 0.1	5.8 ± 0.2	5.3 ± 0.2

[a]Measurements were performed in triplicate with 4 μM protein and 2.5 mM peptide. Values are represented as mean ± standard deviation.

transmembrane proteins DppB and DppC and ultimately result in improved uptake and faster growth at low peptide concentrations (19). To test this hypothesis, DppA variants were purified in their open unliganded conformations, and their binding affinities for different peptides were investigated *in vitro*. To facilitate the purification of DppA, genes harboring the respective mutations were cloned into the expression vector pET30b, generating C-terminal 8×His tag fusions. It was previously reported for the homologous periplasmic binding protein OppA from *E. coli* that fusion to a C-terminal 8×His tag does not affect the binding affinity of the protein for peptide ligands or its solubility (26). The feasibility of this approach for DppA was further supported by the high degree of structural similarity between OppA and DppA (root mean square deviation [RMSD], 2.051 Å over 395 aligned residues; 25.8% sequence identity [27]).

DppA and the S268L and D395dup mutant variants were efficiently synthesized in *E. coli* strain BL21(DE3) and were detectable by SDS-PAGE (Fig. S4a). The T418dup mutant variant was synthesized at much lower levels, presumably due to reduced stability of the protein (see below). Of the double mutants, only the S268L D395dup variant was efficiently synthesized, while the S268L T418dup and D395dup T418dup variants were hardly detectable by SDS-PAGE. Purification of DppA variants by immobilized metal affinity chromatography resulted in highly pure protein fractions (Fig. S4b).

Thermal shift assays with DppA variants. To analyze the thermostabilities of the DppA variants in more detail and to get a first indication of their binding affinities toward peptides, thermal denaturation midpoint shift (T_m shift) assays were performed. In this assay, the apparent midpoint melting temperature (T_m) of thermal denaturation for a protein is determined in the presence and absence of a ligand. Preferential binding of a ligand to the native state of a protein often results in stabilization of the protein by mass action. The difference in T_m between unbound and bound states of a protein (ΔT_m) is often well correlated with binding affinity for ligands binding in the same site with the same binding mode (28). The two ligands tested in these assays were the peptides Ala-γ-Glu-Leu and Ala-γ-Glu-Phe-Leu, which had been used in the previous growth experiments. In the presence of each peptide, the T_m of wild-type DppA was increased, indicating that both peptides bind to the wild-type protein (Table 2 and Fig. 2). All three DppA single mutants were thermally destabilized with respect to the wild-type protein (lower T_m) but exhibited larger ΔT_m values in the presence of either peptide, indicating tighter binding. The largest reduction in T_m of 20.5°C was observed for the T418dup mutant, which also gave the highest ΔT_m values in the presence of peptide. For the S268L D395dup double mutant, a >2-fold higher ΔT_m was detected for both peptides than for the DppA wild type, demonstrating improved binding of peptides containing γ-substituted glutamate residues to this mutant. The S268L T418dup and D395dup T418dup double mutants were hard to purify in sufficient yield and showed no clear denaturation transition or visible precipitate in the tube in the T_m shift assay, and attempts to obtain T_m values by thermal denaturation experiments monitored by circular dichroism spectroscopy were hampered by aggregation. Thus, these double mutants were deemed too unstable for further analysis.

Isothermal titration calorimetry of DppA variants. Isothermal titration calorimetry (ITC) measurements were performed to quantify the binding affinities of DppA

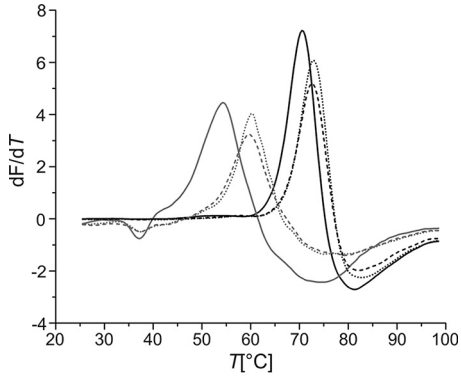

FIG 2 The first derivative of the fluorescence emission as a function of temperature (*dF*/*dT*) from thermal shift assays. The melt curves of wild-type DppA (black) and the mutant variant DppA S268L D395dup (gray) are shown for the unbound proteins (solid lines), when binding to Ala-γ-Glu-Leu (dotted lines), and when binding to Ala-γ-Glu-Phe-Leu (dashed lines). The T_m values are taken from the highest points of the peaks in the derivative plot. Measurements were performed with 4.0 μM protein and 2.5 mM peptide, and the buffer was 50 mM sodium phosphate (pH 7.0).

variants for the two peptide ligands Ala-γ-Glu-Leu and Ala-γ-Glu-Phe-Leu (Table 3). The signal-to-noise ratio in ITC experiments is dependent on the enthalpy change for binding (Δ*H*), which varies with temperature for interactions with nonzero changes in heat capacity and on the amount of ligand that is bound in each injection. Many of the interactions of the peptides with DppA variants were relatively weak in affinity and low in Δ*H*, so it was necessary to maximize the signal-to-noise ratio by using higher protein and ligand concentrations and choosing an experimental temperature where the magnitude of Δ*H* was relatively large for each variant. At the same time, the choice of experimental temperature was limited by the thermal stability of the variants, particularly the less-thermostable mutants T418dup and S268L D395dup, for which experiments were performed only at or below 25°C, outside the region of the thermal denaturation transition. These factors meant that it was not possible to identify a common measurement temperature for all mutants, nor was it possible to measure Δ*H* accurately at a sufficient range of temperatures to obtain the change in heat capacity for binding, so a detailed and unambiguous comparison of thermodynamic parameters

TABLE 3 ITC measurements of DppA variants

DppA wild type or variant by treatment	K_D (μM)[a]	Temp (°C)	No. of expts	*n*	Δ*G* (kcal/mol)	Δ*H* (kcal/mol)[a]	*T*Δ*S* (kcal/mol)
Ala-γ-Glu-Leu							
DppA	3,000[b]	8	1	1[c]	−3.2	4.1	7.3
D395dup	360	37	1	1[c]	−4.9	−6.9	−2.1
S268L	200	37	4	1[c]	−5.2	−4.4	0.9
T418dup	140	25	1	1[c]	−5.3	2.2	7.4
S268L D395dup	6.4	17	1	1.0	−6.9	−7.0	−0.1
S268L D395dup	6.8	25	1	1.1	−7.0	−7.7	−0.7
Ala-γ-Glu-Phe-Leu							
DppA	ND[d]				ND	ND	ND
D395dup	650	37	2	1[c]	−4.5	−2.2	2.3
S268L	110	37	2	1[c]	−5.6	−1.5	4.1
T418dup	15	8	2	1.0	−6.2	0.8	7.0
S268L D395dup	22	17	1	1.0	−6.2	−5.8	0.4
S268L D395dup	23	25	1	1.2	−6.3	−5.5	0.8

[a]The standard errors for K_D and Δ*H* are estimated at 25%, based on the multiple measurements for Ala-γ-Glu-Leu binding to S268L and Ala-γ-Glu-Phe-Leu binding to S268L and T418dup, for which sufficient material was available.
[b]This value is an approximation based on limited data.
[c]*n*, the stoichiometric ratio is fixed at 1 for the fitting of weak binding peptides, as it is not adequately constrained by the data.
[d]ND, not determined.

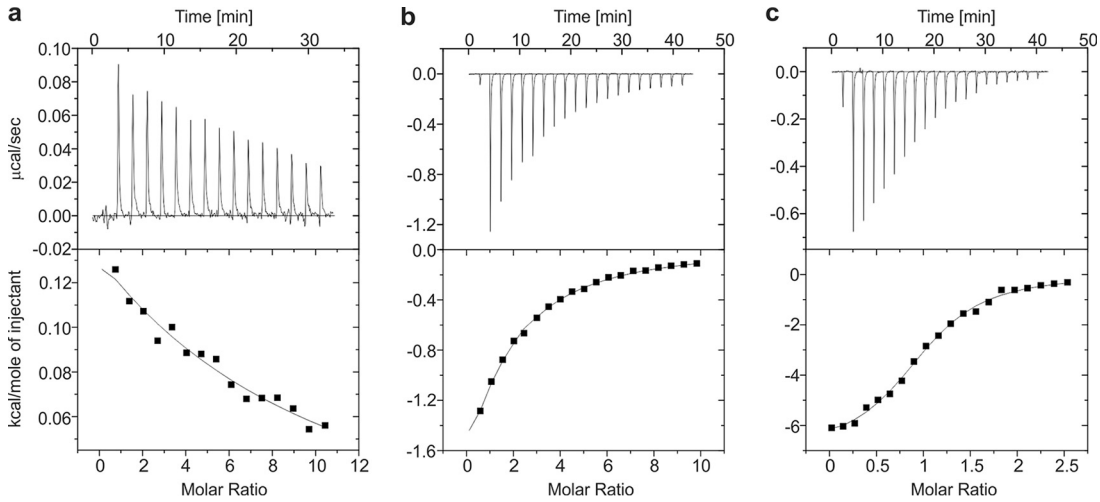

FIG 3 ITC measurements of Ala-γ-Glu-Leu binding to DppA and mutant variants. The upper plots show the differential power versus time for binding reactions upon sequential injections of Ala-γ-Glu-Leu into protein. These data were integrated and normalized to give the heat changes for each injection in kilocalories per mole peptide injected, which are shown as a function of molar ratio (peptide/protein) in the lower plots. The solid lines in the lower plots show the best fit to the data using the One Set of Sites binding model in Origin for ITC. Injections are Ala-γ-Glu-Leu (5 mM) into the DppA (97.5 μM)-containing sample at 8°C (a), Ala-γ-Glu-Leu (5 mM) into the DppA S268L (105 μM)-containing sample at 37°C (b), and Ala-γ-Glu-Leu (0.54 mM) into the DppA S268L D395dup (44.2 μM)-containing sample at 17°C (c). The buffer was 50 mM sodium phosphate (pH 7.0) in all cases.

was not possible. However, the observed trends can easily serve as a qualitative measure to evaluate the effect of the *dppA* mutations on substrate affinity.

Initial ITC experiments with nonrefolded wild-type DppA indicated that only a small fraction of the purified protein was available for binding (15%, according to the fitted binding stoichiometry), which was assumed to be due to copurified peptides bound to DppA. To circumvent this apparent loss of activity, an immobilized metal affinity chromatography (IMAC)-based denaturation and refolding step to remove bound peptides was introduced. ITC experiments with the reference peptides Ala-Thr and Ala-Leu showed that refolded His-tagged DppA exhibited a binding stoichiometry close to the expected value of 1.0 and binding affinities and thermodynamics very similar to the values reported in literature (29), indicating that the C-terminal His tag does not affect binding of the ligand and that the refolded protein is functional (Table S2).

Wild-type DppA bound Ala-γ-Glu-Leu only weakly, with a dissociation constant (K_D) of approximately 3 mM (Table 3). The three DppA single mutants had higher affinities toward Ala-γ-Glu-Leu, as indicated by 9- to 22-fold reduction in the K_D value, in agreement with the results from the thermal shift assays. The highest binding affinity toward Ala-γ-Glu-Leu was measured for the S268L D395dup double mutant, resulting in a K_D value of 6 μM, constituting an approximately 500-fold improvement in affinity compared to wild-type DppA. Representative ITC data showing the improvement in affinity for the DppA S268L and S268L D395dup variants are shown in Fig. 3.

In the case of the peptide Ala-γ-Glu-Phe-Leu, binding to wild-type DppA was apparently too weak to measure, but affinity was again improved upon mutation, resulting in K_D values of around 20 μM for variants T418dup and S268L D395dup, approximately 7-fold stronger and 3-fold weaker than the respective affinities of these variants for Ala-γ-Glu-Leu. Given that the enthalpy of ionization for phosphate buffer is relatively small at the experimental temperatures used, meaningful comparisons of binding enthalpy can be made for measurements at the same temperature. For all mutants where such a comparison could be made, the binding of Ala-γ-Glu-Phe-Leu was less enthalpically favorable (less-negative ΔH) but more entropically favorable (more-positive $T\Delta S$) than the binding of Ala-γ-Glu-Leu, probably reflecting the increased contribution of hydrophobic interactions in the binding of the phenylalanine-containing ligand.

These findings showed that the size and structure of the cargo molecule attached to the glutamate side chain seem to have only a small impact on the binding efficiencies of peptides to these DppA mutant variants, which together with the less efficient hydrolysis of the cleavage product γ-Glu-Phe-Leu by *Pn*GGT explains the higher Ala-γ-Glu-Phe-Leu concentrations needed for growth of the leucine auxotrophic selection strain.

Uptake of phosphorylated cargo molecules. Finally, we wondered whether the changes in DppA that improved transport of bulky molecules, such as Ala-γ-Glu-Phe-Leu, might coincidentally also improve uptake of heavily negatively charged molecules, such as phosphorylated cargo molecules. For that, the threonine biosynthesis pathway intermediate *O*-phospho-L-homoserine (PHS) and the noncanonical amino acid *O*-phospho-L-serine (SEP), which can be site-specifically incorporated into proteins to study the effects of protein phosphorylation (30), were attached to the glutamate side chain of the peptide Ala-Glu (Fig. 1a, peptides 3 and 4). Unfortunately, simultaneous synthesis of *Pn*GGT and a DppA wild type or mutant variant in the threonine auxotrophic strain TK074 did not restore growth of this strain in minimal medium supplemented with 2 mM Ala-γ-Glu-PHS. Subsequent thermal shift assays with wild-type DppA and the DppA D395dup mutant revealed only minimal binding of the two peptides containing the phosphorylated cargo molecules to the DppA variants (Fig. S5). These results indicate that uptake of the two peptides is most likely prevented by insufficient recognition by DppA and that new DppA variants would need to be evolved to expand import to such molecules.

DISCUSSION

In this study, three mutant variants of the periplasmic substrate-binding protein DppA were identified that led to improved utilization of peptides containing γ-substituted glutamate residues. These peptides are of particular interest, as they can be used as transport vectors in a previously described synthetic transport system (9). This system provides a novel way to make compounds available in the cytoplasm of *E. coli* that are otherwise not taken up by the cell, thereby offering a valuable tool for metabolic engineering and synthetic biology approaches.

DppA is part of the dipeptide permease transport system that was shown by mutational studies to be responsible for the uptake of the peptide Ala-γ-Glu-Leu. Thermal denaturation midpoint shift assays and isothermal titration calorimetry revealed that all three mutations that were identified in DppA significantly increased the affinity for the peptides Ala-γ-Glu-Leu and Ala-γ-Glu-Phe-Leu, leading to improved uptake and eventually faster growth on these substrates, but not for the phosphorylated peptides Ala-γ-Glu-PHS and Ala-γ-Glu-SEP. In general, DppA is known to be more restrictive toward side-chain modifications of its peptide substrates than the SBP OppA of the oligopeptide permease transport system (23). Elucidation of the DppA crystal structure in complex with the substrate Gly-Leu revealed that the substrate-binding site of DppA contains two pockets, a larger pocket accommodating the side chain of the N-terminal amino acid, and a smaller pocket accommodating the side chain of the C-terminal amino acid of a peptide substrate (21). The smaller size of the second pocket might explain the lower tolerance of wild-type DppA for side-chain modifications in general and the low affinity for peptides containing γ-glutamyl amides in this position in particular. The crystal structure of wild-type DppA also revealed that the smaller pocket is delineated by residues Thr20, Ser21, Trp386, Tyr389, Leu390, Met403, Trp405, Ser429, and Tyr431. Interestingly, the two amino acid insertions in the identified DppA variants are duplications of residues Asp395 and Thr418 and therefore lie in the same domain and in close proximity to most of the residues delineating the pocket that accommodates the γ-substituted glutamate residue (Fig. S6). These findings suggest that the insertions might lead to conformational changes that facilitate the binding of γ-glutamyl amides in this pocket. Residue Ser268, on the other hand, is part of strand β5-III, a β-sheet that is antiparallel to strand β3-III, which is, again, antiparallel to the

peptide ligand and strongly involved in its binding. Therefore, mutation S268L might, although indirectly, influence the binding of certain peptide ligands.

Our results indicate that the tolerance of DppA for certain side-chain modifications can be significantly increased by introducing point mutation S268L or duplicating residues D395 or T418. These findings are consistent with the assumption that for the Dpp system, the SBP of the ABC transporter primarily determines the specificity of the entire transporter, as is the case for other ABC transporters as well (15, 19, 20, 31, 32). To grow a leucine auxotrophic selection strain on minimal medium containing Ala-γ-Glu-Phe-Leu, higher peptide concentrations were required than for minimal medium containing Ala-γ-Glu-Leu. It is likely that slower growth on Ala-γ-Glu-Phe-Leu is largely attributable to less efficient hydrolysis of γ-Glu-Phe-Leu by *Pn*GGT after transport, as consistent with kinetic measurements with purified *Pn*GGT. This finding offers the potential to further improve the synthetic transport system in future work by broadening the substrate specificity of *Pn*GGT by directed evolution. Other possible explanations for the inefficient utilization of Ala-γ-Glu-Phe-Leu include impaired removal of the N-terminal alanine residue to make γ-Glu-Phe-Leu available for *Pn*GGT or slower hydrolysis of Phe-Leu by the peptidases of *E. coli*. The finding that peptides containing phosphorylated cargo molecules were not sufficiently bound by DppA can be explained by the small size of the second DppA binding pocket or, more likely, by the negative charge of the attached phosphate group. Accommodating the negative charges in the rather narrow binding pocket of DppA would presumably require more extensive restructuring of the binding pocket, which was unlikely to be achieved with the selection strategy that was used to identify the DppA mutant variants described in this study.

A comparison of ITC data with previously published values for the interaction of dipeptides with wild-type DppA shows that the strongest affinity achieved in this study for variant S268L D395dup with the peptide Ala-γ-Glu-Leu (7 μM, ΔH −7.7 kcal/mol at 25°C) is comparable to that observed for the weakest binding standard dipeptide studied previously with wild-type DppA (6 μM, ΔH −10.3 kcal/mol) (29). The fact that the binding is less enthalpically favorable but more entropically favorable for variant S268L D395dup can presumably be explained by the displacement of additional water by the larger and more hydrophobic ligand. The majority of dipeptides studied showed significantly higher affinity for DppA (in the nM range) and more exothermic enthalpies of binding, evincing the evolutionary optimization of the whole binding site for dipeptide binding.

Two out of the three DppA mutant variants we identified resulted from the duplication of single codons, presumably introduced by replication slippage (33), demonstrating that the introduction of insertions can be a valid approach to improve protein function. Even though we cannot exclude that a similar effect might have been achieved without duplication by saturation mutagenesis of one or several amino acid residues at the site of the duplicated codon, we can state that extension resulted as a suitable outcome that would have been difficult to achieve with other standard directed evolution methods, such as error-prone PCR, as these do not address the length of a sequence. Only recently, a directed evolution method for the generation of libraries that vary both in sequence and length was developed, which could have potentially produced similar mutations (34).

Taken together, our data demonstrate that the affinity of an ABC transporter for a ligand can be significantly improved by mutating the substrate-binding protein of the transporter. This finding greatly improves the efficiency and applicability of the *Pn*GGT-based synthetic transport system and additionally offers the potential to improve previous peptide-based approaches to overcome transport problems (3, 5–8).

MATERIALS AND METHODS

Strains and media. All bacterial strains used in this study are listed in Table 4. For cloning purposes, *E. coli* strain DH5α λpir was used. The *dppABCDF* and *oppABCDF* operons were deleted by plasmid-based gene replacement (35, 36). For this, two 500-bp fragments flanking the respective operon were amplified, combined by PCR, and cloned into plasmid pEMG via EcoRI and BamHI (both New England BioLabs,

TABLE 4 Strains used in this study

E. coli strain	Description	Reference(s) or source
DH5α λ*pir*	*supE44* Δ*lacU169* (ϕ80*lacZ*ΔM15) *hsdR17* (r_K^- m_K^+) *recA1 endA1 thi-1 gyrA relA* lysogenic λ*pir*	50
JM101	*glnV44 thi-1* Δ(*lac-proAB*) F′[*lacI*^{q}*Z*ΔM15 *traD36 proAB*$^+$]	51, 52
BL21(DE3)	*E. coli* strain B F$^-$ *ompT gal dcm lon hsdS*$_B$(r_B^- m_B^-) λ(DE3 [*lacI lacUV5-T7p07 ind1 sam7 nin5*]) [*malB*$^+$]$_{K\text{-}12}$(λ^S)	53
JW0002	BW25113 *thrB*::*kan*	37
TK060	JM101 Δ*ggt* Δ*pcnB*	This study
TK070 (TK054 Δ*pcnB*)	JM101 Δ*leuB* Δ*ggt* Δ*liv* Δ*brnQ* Δ*pcnB*	9
TK071	TK070 Δ*dppABCDF*	This study
TK072	TK070 Δ*oppABCDF*	This study
TK073	TK070 Δ*dppABCDF* Δ*oppABCDF*	This study
TK074	TK060 Δ*thrB*	This study

Ipswich, MA, USA) restriction sites. For the construction of strains TK060 and TK074, the *ggt*, *pcnB*, and *thrB* genes were replaced with disrupted versions by P1 phage transduction using the respective donor strains from the KEIO collection (37, 38).

Bacterial cultures were grown in LB Miller broth (Becton Dickinson, Sparks, MD, USA) or super optimal broth (SOB) medium as standard growth media (39, 40). Growth experiments in selective medium were carried out in M9 minimal medium (40) containing 0.5% glucose and different concentrations of the peptides alanyl-γ-glutamyl-leucine (Ala-γ-Glu-Leu), alanyl-γ-glutamyl-phenylalanyl-leucine (Ala-γ-Glu-Phe-Leu), and alanyl-γ-glutamyl-PHS, as described previously (9). Ala-γ-Glu-Leu and Ala-γ-Glu-Phe-Leu were custom synthesized by Pepscan (>95% purity; Lelystad, The Netherlands). For the preparation of solid medium, Bacto agar (Becton Dickinson) was added to a final concentration of 1.5%. Antibiotics were added to all media to obtain the following concentrations: kanamycin, 50 $\mu g \cdot ml^{-1}$; chloramphenicol, 34 $\mu g \cdot ml^{-1}$; gentamicin, 10 $\mu g \cdot ml^{-1}$; and carbenicillin, 100 $\mu g \cdot ml^{-1}$.

Chemical synthesis of Ala-γ-Glu-PHS and Ala-γ-Glu-SEP. The benzyl-protected phosphoserine methyl ester hydrochloride molecule 6 or its phosphohomoserine congener molecule 7 were coupled with peptide 5 using *O*-benzotriazole-*N*,*N*,*N*′,*N*′-tetramethyluronium hexafluorophosphate (HBTU) as the coupling agent (Fig. 4). This provided us with the fully protected dipeptides 8 and 9 in good yields. Peptide 8 was initially subjected to ester hydrolysis to cleave the methyl esters. Subsequent N-terminal deprotection followed by catalytic hydrogenation provided us with a dephosphorylated peptide. We next tried to deprotect the phosphate group after ester hydrolysis but before carbamate deprotection and again obtained, as the sole product, a peptide in which the phosphate group had been cleaved.

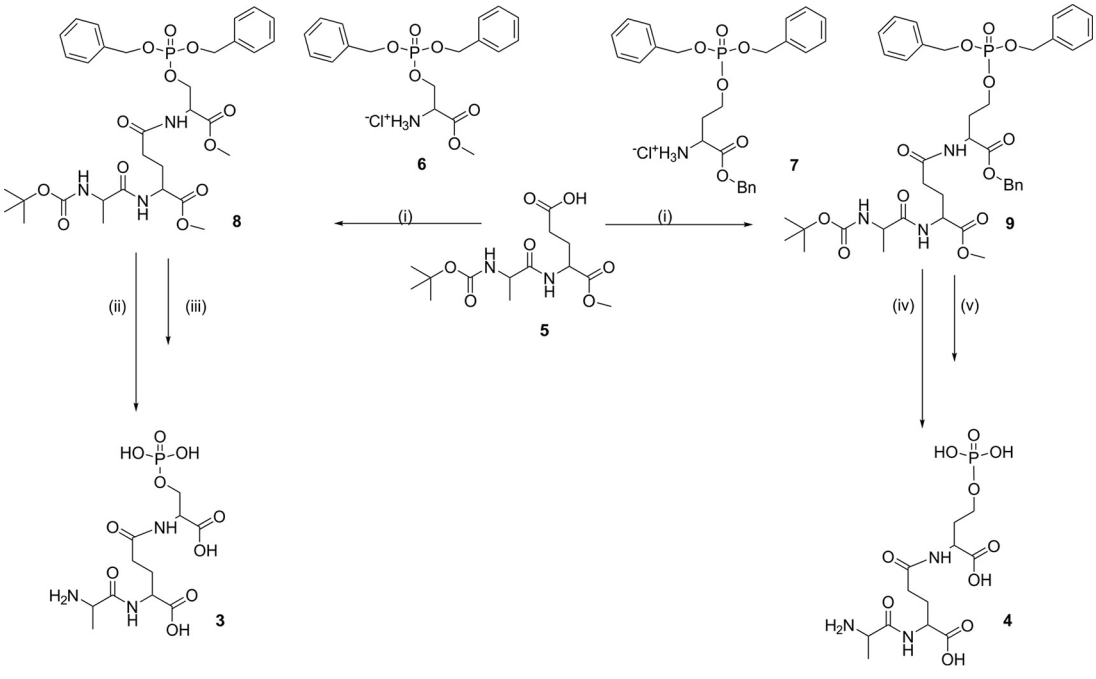

FIG 4 Synthesis scheme for Ala-γ-Glu-SEP (peptide 3) and Ala-γ-Glu-PHS (peptide 4). The Materials and Methods section contains a detailed description of the synthesis routes.

TABLE 5 Plasmids used in this study

Plasmid	Description[a]	Reference or source
pACT3	Expression vector; pLlacO1 *p15A ori* Cm^r *lacI^q*	54
pSEVA271	MCS; pSC101 *ori* Kan^r	55
pAB92	SEVA vector backbone; MCS, pBR322 *ori* Amp^r, P_{tet}-P_{T7} fusion promoter	56
pET30b	T7 promoter; MCS; pBR322 *ori*, Kan^r	Novagen (Madison, WI, USA)
pEMG	Delivery vector for plasmid-based gene replacement; *oriR6K lacZ*α, flanking I-SceI sites, Kan^r	35
p*ParaI-SceI*	I-SceI gene under the control of L-arabinose-inducible promoter; p15A *ori*, Gm^r	57
p*Pn*GGT (pACT3/6×His_ *Pn*GGT ΔN24)	*Pn*GGT ΔN24 gene with N-terminal MRGSHHHHHHGSACEL cloned in pACT3	9
pEMG-*dppABCDF*	pEMG bearing a 1.0-kb TS1-TS2 EcoRI-BamHI insert for deleting *dppABCDF*	This study
pEMG-*oppABCDF*	pEMG bearing a 1.0-kb TS1-TS2 EcoRI-BamHI insert for deleting *oppABCDF*	This study
pSEVA271/*dppA*	pSEVA271 backbone with P_{tet}-P_{T7} fusion promoter fragment from pAB92 and *dppA* gene	This study
pSEVA271/*dppA*_S268L	pSEVA271/*dppA* with S268L mutation	This study
pSEVA271/*dppA*_D395dup	pSEVA271/*dppA* with duplication of residue D395	This study
pSEVA271/*dppA*_S268L_D395dup	pSEVA271/*dppA* with S268L mutation and duplication of residue D395	This study
pET30b/dppA	pET30b containing *dppA* gene with C-terminal 8×His tag pET30b	This study
pET30b/*dppA*_S268L	pET30b/*dppA* with S268L mutation	This study
pET30b/*dppA*_D395dup	pET30b/*dppA* with duplication of residue D395	This study
pET30b/*dppA*_T418dup	pET30b/*dppA* with duplication of residue T418	This study
pET30b/*dppA*_S268L_D395dup	pET30b/*dppA* with S268L mutation and duplication of residue D395	This study
pET30b/*dppA*_S268L_T418dup	pET30b/*dppA* with S268L mutation and duplication of residue T418	This study
pET30b/*dppA*_D395dup_T418dup	pET30b/*dppA* with duplication of residue D395 and duplication of residue T418	This study

[a]Cm^r, chloramphenicol resistance; Kan^r, kanamycin resistance; MCS, multicloning site; Amp^r, ampicillin resistance; Gm^r, gentamicin resistance.

Phosphate deprotection with the methyl ester still in place, however, gave us the phosphorylated peptide in good yield. It seems that the alpha-carboxylate of the serine residue is involved in the phosphate ester hydrolysis during catalytic hydrogenation wherein the carboxylate attacks the phosphate center structure resulting in dephosphorylation. This hypothesis is supported by the results obtained during deprotection of peptide 3. The α-benzyl ester and the benzyl phosphates can be easily deprotected in one-pot hydrogenation. In this case (peptide 9), a good yield of completely deprotected peptide 4 was obtained after acid hydrolysis of carbamate and ester cleavage of glutamate. Thereafter, peptide 8 was first subjected to acid, followed by hydrogenation and then ester deprotection to obtain phosphorylated peptide 3. After complete deprotection, the peptides were purified on a reverse-phase high-performance liquid chromatogram (RP-HPLC; water-acetonitrile–0.1% trifluoroacetic acid [TFA]) to obtain peptides 3 and 4 as white solids in trifluoroacetate form.

The reagents and conditions used were (i) dry dimethylformamide (DMF), HBTU, and *N*,*N*-diisopropylethylamine (DIPEA) at 0°C to room temperature (r.t.) overnight; (ii) 50% TFA in DCM for 8 h, followed by 10% Pd(0)/C and H_2O:CH_3OH at 1:1 in H_2 overnight; (iii) LiOH and H_2O:CH_3OH at 1:1 overnight, with the reaction quenched with CH_3COOH; (iv) 10% Pd(0)/C, H_2O:CH_3OH at 1:1, and H_2 overnight; and (v) 50% TFA in DCM for 8 h, followed by LiOH and H_2O:CH_3OH at 1:1 overnight, with the reaction quenched with CH_3COOH.

All moisture-sensitive reactions were performed under a nitrogen atmosphere. Dry solvents were purchased from commercial sources and used as such. Reactions were monitored by thin-layer chromatography (TLC; precoated silica gel plate F254; Merck Millipore, Billerica, MA, USA). Flash chromatography was done on Merck Kieselgel 60 (230 to 400 mesh). ^{1}H, ^{13}C, and ^{31}P spectra were recorded on nuclear magnetic resonance (NMR) spectrometers operating at 300 MHz, 75 MHz, and 121 MHz, respectively (see the supplemental material).

DNA constructs. For cloning purposes, DNA fragments were amplified using Phusion high-fidelity DNA polymerase (New England BioLabs). Derivatives of plasmids pEMG and pET30b were constructed by conventional cloning using restriction enzymes and a Quick Ligation kit (all New England BioLabs). Derivatives of plasmid pSEVA271 were constructed by Gibson Assembly (New England BioLabs) using the vector backbone of pSEVA271, the P_{tet}-P_{T7} fusion promoter from plasmid pAB92, and the *dppA* gene amplified from chromosomal *E. coli* DNA. DNA constructs were verified by Sanger sequencing (Microsynth, Balgach, Switzerland) and are summarized in Table 5. The oligonucleotides used for construction are listed in Table 6.

Protein synthesis and purification. To synthesize *Pn*GGT in strain JM101 and the DppA variants in BL21(DE3), cells carrying the respective plasmids were grown in LB medium to an optical density at 600 nm (OD_{600}) of approximately 0.5 and induced with 0.5 mM IPTG. Following an expression period (20 h, 20°C), cells were harvested by centrifugation, resuspended in lysis buffer (50 mM NaH_2PO_4, 300 mM NaCl, 10 mM imidazole, 1 mg · ml^{-1} lysozyme [pH 8.0]), incubated for 30 min on ice, and then frozen at −80°C for at least 30 min. After thawing and subsequent centrifugation, the supernatant containing the soluble protein fraction was collected.

His-tagged *Pn*GGT was purified by immobilized metal affinity chromatography (IMAC) using nickel-nitrilotriacetic acid (Ni-NTA) Superflow (Qiagen, Hilden, Germany), as described previously (41). Fractions containing purified *Pn*GGT were dialyzed against 50 mM Tris-HCl (pH 7.0). To obtain DppA variants in

TABLE 6 Oligonucleotides used in this study

Oligonucleotide name	Sequence[a]	Description (restriction enzyme)
TK335	ATATGAATTCGAGCACCTGCACGGCAC	TS1F primer for plasmid-based gene replacement of *oppABCDF* (EcoRI)
TK336	GGGCTGACAACTGTCAGCCCTCATCCTCATGAGCTGCAGATGC	TS1R primer for plasmid-based gene replacement of *oppABCDF*
TK337	GCATCTGCAGCTCATGAGGATGAGGGCTGACAGTTGTCAGCCC	TS2F primer for plasmid-based gene replacement of *oppABCDF*
TK338	ATATGGATCCGCTCGATGCCCGTTTATGGC	TS2R primer for plasmid-based gene replacement of *oppABCDF* (BamHI)
TK339	ATATGAATTCGTGGCGAGTAATCCTCTATCACCG	TS1F primer for plasmid-based gene replacement of *dppABCDF* (EcoRI)
TK340	CATGGCCCCGGTTTTGTGAGCCGGGATTTACACCAACGGTG	TS1R primer for plasmid-based gene replacement of *dppABCDF*
TK341	CACCGTTGGTGTAAATCCCGGCTCACAAAACCGGGGCCATG	TS2F primer for plasmid-based gene replacement of *dppABCDF*
TK342	ATATGGATCCGCCACGAAGAAGCCGTTTCTG	TS2R primer for plasmid-based gene replacement of *dppABCDF* (BamHI)
TK410	ATATCATATGCGTATTTCCTTGAAAAAGTCAGGGATGC	Forward primer for amplification of *dppA* for cloning in pET30b (NdeI)
TK411	ATATGGATCCCTACTAGTGGTGGTGGTGGTGGTGGTGTTCGATAGAGACGTTTTCGAAGTGATG	Reverse primer for amplification of *dppA* with C-terminal 8×His tag for cloning in pET30b (BamHI)
TK446	AGACTAGTCGCCAGGGTTTTCCCAGTCACG CTAGTGCTTAAGACCCACTTTC	Forward primer for amplification of P_{tet}-P_{T7} promoter from pAB92 for Gibson Assembly of pSEVA271/*dppA* derivatives
TK447	CATCCCTGACTTTTTCAAGGAAATACGCATAAGCTTATATCTCCTTCTTAAAG	Reverse primer for amplification of P_{tet}-P_{T7} promoter from pAB92 for Gibson Assembly of pSEVA271/*dppA* derivatives
TK448	CATCACTTCGAAAACGTCTCTATCGAATAAGGCCTCCTGTGTGAAATTGTTATCC	Forward primer for amplification of pSEVA271 backbone for Gibson Assembly of pSEVA271/*dppA* derivatives
TK449	TAAATGTGAAAGTGGGTCTTAAGCACTAGCGTGACTGGGAAAACCCTGG	Reverse primer for amplification of pSEVA271 backbone for Gibson Assembly of pSEVA271/*dppA* derivatives
TK450	TGTTTAACTTTAAGAAGGAGATATAAGCTTATGCGTATTTCCTTGAAAAAGTCAGGG	Forward primer for amplification of *dppA* from genomic DNA for Gibson Assembly of pSEVA271/*dppA* derivatives
TK451	AAAGCGGATAACAATTTCACACAGGAGGCCTTATTCGATAGAGACGTTTTCGAAGTGATG	Reverse primer for amplification of *dppA* from genomic DNA for Gibson Assembly of pSEVA271/*dppA* derivatives
TK471	CGTCGGTTATCTCTTGTATAACGTGCAGAAAAAACC	Forward primer for introducing S268L mutation in DppA
TK472	GGTTTTTTCTGCACGTTATACAAGAGATAACCGACG	Reverse primer for introducing S268L mutation in DppA
TK473	GGATAACTTCTTCGCCACCACCCTGTTCAGCTGCGCCG	Forward primer for introducing T418dup mutation in DppA
TK474	CGGCGCAGCTGAACAGGGTGGTGGCGAAGAAGTTATCC	Reverse primer for introducing T418dup mutation in DppA
TK475	CCTCAAGCGTGCGAAAGATGATGGCGAGCACCAGACGG	Forward primer for introducing D395dup mutation in DppA
TK476	CCGTCTGGTGCTCGCCATCATCTTTCGCACGCTTGAGG	Reverse primer for introducing D395dup mutation in DppA

[a]Restriction sites are underlined.

their open unliganded conformation, proteins were immobilized on a column containing Ni-NTA Superflow and were partly denatured and refolded by washing with washing buffer (50 mM 4-morpholineethanesulfonic acid, 300 mM NaCl, and 20 mM imidazole [pH 8] containing decreasing concentrations of guanidinium hydrochloride [4 column volumes {CV} of 2 M, 4 CV of 1.5 M, 4 CV of 1 M, 4 CV of 0.5 M, and 10 CV of buffer without guanidinium hydrochloride]) (26). The refolded protein was eluted in 7 steps with elution buffer (50 mM 4-morpholineethanesulfonic acid, 300 mM NaCl, and 500 mM imidazole [pH 6]). Subsequent to purification, fractions containing DppA variants were dialyzed three times against a 1,000-fold excess of 50 mM sodium phosphate buffer (pH 7.0) and filtered using Millex-GV 0.22-μm-pore-size polyvinylidene difluoride (PVDF) syringe filters (Merck Millipore) to remove larger particles. The concentrations of DppA variants were determined by UV absorption at 280 nm with an HP 8453 UV spectroscope (Hewlett-Packard, Palo Alto, CA, USA), by using the calculated molar extinction coefficient (ε) of 89,980 $M^{-1} \cdot cm^{-1}$ (42). All protein samples were analyzed by SDS-PAGE, as reported previously (43).

Kinetic measurements with *Pn*GGT. To determine the kinetic properties of *Pn*GGT, appropriate amounts of purified protein were preincubated at 37°C in 50 mM Tris-HCl (pH 7.0). To start the reaction, the substrate γ-Glu-Leu (Bachem, Bubendorf, Switzerland) or γ-Glu-Phe-Leu (custom synthesized to >95% purity, Pepscan, Lelystad, Netherlands) was added at the indicated concentrations. The reaction was stopped at different time points by mixing 100 μl of the reaction mix with 100 μl of 50 mM Tris-HCl (pH 7.0) preheated to 95°C and shaking at 600 rpm. After 5 min of incubation at 95°C, the samples were centrifuged at 4°C and 21,130 × *g* to remove the denatured protein. The supernatant was diluted in 50 mM Tris-HCl (pH 7.0) as necessary, and the glutamate concentration was determined using a commercial enzyme assay (glutamate assay kit [fluorometric]; Abcam, Cambridge, United Kingdom). Data from measurements were analyzed using SigmaPlot 12.2 (Systat, San Jose, CA, USA).

Thermal shift assay. The thermal denaturation midpoint melting temperature (T_m) of DppA wild-type protein and variants was determined by monitoring the fluorescence intensity of Sypro Orange dye in the absence/presence of peptides as a function of temperature. Protein was mixed with 1× Sypro Orange from Thermo Fisher Scientific (Waltham, MA, USA) in 50 mM sodium phosphate (pH 7.0). The experiments were performed with a real-time PCR system (Rotor-Gene Q; Qiagen, Hilden, Germany) with a temperature ramp from 25 to 95°C, using a ramp rate of 5.3°C · min^{-1} and a reaction volume of 40 μl. The first derivative of the fluorescence intensity curve was calculated in order to determine the midpoint melting temperature (T_m) for proteins with and without bound peptides.

Isothermal titration calorimetry. ITC was performed using the MicroCal ITC-200 instrument (Malvern Instruments, Worcestershire, UK). The cell volume was 200 μl, and each injection volume was 2 μl. Peptide and protein concentrations were chosen for each mutant and peptide to give data suitable for accurate K_D determination. All measurements were conducted in 50 mM sodium phosphate (pH 7.0) as a buffer. Solutions were degassed under a vacuum for 10 min prior to the experiments. Peptide solutions in the injection syringe were titrated into the calorimeter cell-containing protein solutions, and the heat flow caused by protein-peptide interaction was recorded and analyzed by the software provided with the instrument. The quantitative interpretation of the binding isotherm was performed with the "One Sets of Sites" binding model in the MicroCal Origin software (OriginLab, Northampton, MA, USA).

Genome sequencing of mutant strains. In order to prepare chromosomal DNA for resequencing, genomic DNA was purified with the High Pure PCR template preparation kit (Roche Diagnostics, Basel, Switzerland). Sequencing libraries were prepared using TruSeq DNA sample preparation kit version 2 (Illumina, San Diego, CA, USA). These libraries were then purified using 0.7× volumes of Agencourt AMPure XP beads (Beckman Coulter, Pasadena, CA, USA) to exclude very short library fragments. For sequencing the purified libraries, MiSeq (Illumina) paired-end (PE) 2 × 301 cycles was used with the 600-cycle version 3 kit and converted to fastq files. Reads were aligned using the Bowtie 2 package (44, 45). Sequences were analyzed using the deepSNV package (46, 47) and Integrated Genome Viewer (48, 49).

SUPPLEMENTAL MATERIAL

Supplemental material for this article may be found at https://doi.org/10.1128/AEM.00340-18.

SUPPLEMENTAL FILE 1, PDF file, 1.0 MB.

ACKNOWLEDGMENTS

We thank Tania Roberts and Sibylle Schmitter for critical reading of the manuscript, Philippe Marlière for valuable discussions, and Christian Beisel, Manuel Kohler, and the Quantitative Genomics Facility (D-BSSE, ETH Zurich) for next-generation sequencing.

This work was supported by the European Commission (FP7, grant 289572-METACODE).

REFERENCES

1. Kell DB, Swainston N, Pir P, Oliver SG. 2015. Membrane transporter engineering in industrial biotechnology and whole cell biocatalysis. Trends Biotechnol 33:237–246. https://doi.org/10.1016/j.tibtech.2015.02.001.

2. Ames BN, Ames GF, Young JD, Tsuchiya D, Lecocq J. 1973. Illicit transport: the oligopeptide permease. Proc Natl Acad Sci U S A 70:456–458.

3. Boehm JC, Kingsbury WD, Perry D, Gilvarg C. 1983. The use of cysteinyl peptides to effect portage transport of sulfhydryl-containing compounds in *Escherichia coli*. J Biol Chem 258:14850–14855.
4. Fickel TE, Gilvarg C. 1973. Transport of impermeant substances in *E. coli* by way of oligopeptide permease. Nat New Biol 241:161–163. https://doi.org/10.1038/newbio241161a0.
5. Hong NJ, Park YT. 1993. Portage transport of toxophoric agent, *N*-hydroxyalanine, through oligopeptide permease in *Escherichia coli*. Bull Korean Chem Soc 14:674–678.
6. Hwang SY, Berges DA, Taggart JJ, Gilvarg C. 1989. Portage transport of sulfanilamide and sulfanilic acid. J Med Chem 32:694–698. https://doi.org/10.1021/jm00123a034.
7. Kingsbury WD, Boehm JC, Mehta RJ, Grappel SF, Gilvarg C. 1984. A novel peptide delivery system involving peptidase activated prodrugs as antimicrobial agents. Synthesis and biological activity of peptidyl derivatives of 5-fluorouracil. J Med Chem 27:1447–1451.
8. Kingsbury WD, Boehm JC, Perry D, Gilvarg C. 1984. Portage of various compounds into bacteria by attachment to glycine residues in peptides. Proc Natl Acad Sci U S A 81:4573–4576.
9. Kuenzl T, Sroka M, Srivastava P, Herdewijn P, Marliere P, Panke S. 2017. Overcoming the membrane barrier: recruitment of gamma-glutamyl transferase for intracellular release of metabolic cargo from peptide vectors. Metab Eng 39:60–70. https://doi.org/10.1016/j.ymben.2016.10.016.
10. Wilkens S. 2015. Structure and mechanism of ABC transporters. F1000Prime Rep 7:14. https://doi.org/10.12703/P7-14.
11. Maqbool A, Horler RS, Muller A, Wilkinson AJ, Wilson KS, Thomas GH. 2015. The substrate-binding protein in bacterial ABC transporters: dissecting roles in the evolution of substrate specificity. Biochem Soc Trans 43:1011–1007. https://doi.org/10.1042/BST20150135.
12. Linton KJ, Higgins CF. 1998. The *Escherichia coli* ATP-binding cassette (ABC) proteins. Mol Microbiol 28:5–13. https://doi.org/10.1046/j.1365-2958.1998.00764.x.
13. Payne JW. 2008. Transport and hydrolysis of peptides by microorganisms, p 305–334. *In* Elliott M, O'Connor M (ed), Ciba Foundation symposium 50: peptide transport and hydrolysis. John Wiley & Sons, Hoboken, NJ.
14. Alves RA, Payne JW. 1980. The number and nature of the peptide-transport systems of *Escherichia coli*: characterization of specific transport mutants. Biochem Soc Trans 8:704–705. https://doi.org/10.1042/bst0080704a.
15. Smith MW, Tyreman DR, Payne GM, Marshall NJ, Payne JW. 1999. Substrate specificity of the periplasmic dipeptide-binding protein from *Escherichia coli*: experimental basis for the design of peptide prodrugs. Microbiology 145:2891–2901. https://doi.org/10.1099/00221287-145-10-2891.
16. Payne JW. 1968. Oligopeptide transport in *Escherichia coli*. Specificity with respect to side chain and distinction from dipeptide transport. J Biol Chem 243:3395–3403.
17. Payne JW, Gilvarg C. 1968. Size restriction on peptide utilization in *Escherichia coli*. J Biol Chem 243:6291–6299.
18. Smith RL, Archer EG, Dunn FW. 1970. Uptake of [^{14}C]-labeled tri-, tetra-, and pentapeptides of phenylalanine and glycine by *Escherichia coli*. J Biol Chem 245:2967–2971.
19. Doeven MK, Abele R, Tampe R, Poolman B. 2004. The binding specificity of OppA determines the selectivity of the oligopeptide ATP-binding cassette transporter. J Biol Chem 279:32301–32307. https://doi.org/10.1074/jbc.M404343200.
20. Doeven MK, Kok J, Poolman B. 2005. Specificity and selectivity determinants of peptide transport in *Lactococcus lactis* and other microorganisms. Mol Microbiol 57:640–649. https://doi.org/10.1111/j.1365-2958.2005.04698.x.
21. Dunten P, Mowbray SL. 1995. Crystal structure of the dipeptide binding protein from *Escherichia coli* involved in active transport and chemotaxis. Protein Sci 4:2327–2334. https://doi.org/10.1002/pro.5560041110.
22. Tame JR, Dodson EJ, Murshudov G, Higgins CF, Wilkinson AJ. 1995. The crystal structures of the oligopeptide-binding protein OppA complexed with tripeptide and tetrapeptide ligands. Structure 3:1395–1406. https://doi.org/10.1016/S0969-2126(01)00276-3.
23. Perry D, Gilvarg C. 1984. Spectrophotometric determination of affinities of peptides for their transport systems in *Escherichia coli*. J Bacteriol 160:943–948.
24. Tavori H, Kimmel Y, Barak Z. 1981. Toxicity of leucine-containing peptides in *Escherichia coli* caused by circumvention of leucine transport regulation. J Bacteriol 146:676–683.
25. Dragosits M, Mattanovich D. 2013. Adaptive laboratory evolution–principles and applications for biotechnology. Microb Cell Fact 12:64–64. https://doi.org/10.1186/1475-2859-12-64.
26. Klepsch MM, Kovermann M, Low C, Balbach J, Permentier HP, Fusetti F, de Gier JW, Slotboom DJ, Berntsson RP. 2011. *Escherichia coli* peptide binding protein OppA has a preference for positively charged peptides. J Mol Biol 414:75–85. https://doi.org/10.1016/j.jmb.2011.09.043.
27. Konagurthu AS, Whisstock JC, Stuckey PJ, Lesk AM. 2006. MUSTANG: a multiple structural alignment algorithm. Proteins 64:559–574. https://doi.org/10.1002/prot.20921.
28. Fedorov O, Niesen FH, Knapp S. 2012. Kinase inhibitor selectivity profiling using differential scanning fluorimetry. Methods Mol Biol 795:109–118. https://doi.org/10.1007/978-1-61779-337-0_7.
29. Payne JW, Grail BM, Gupta S, Ladbury JE, Marshall NJ, O'Brien R, Payne GM. 2000. Structural basis for recognition of dipeptides by peptide transporters. Arch Biochem Biophys 384:9–23. https://doi.org/10.1006/abbi.2000.2084.
30. Rogerson DT, Sachdeva A, Wang K, Haq T, Kazlauskaite A, Hancock SM, Huguenin-Dezot N, Muqit MMK, Fry AM, Bayliss R, Chin JW. 2015. Efficient genetic encoding of phosphoserine and its non-hydrolyzable analog. Nat Chem Biol 11:496–503. https://doi.org/10.1038/nchembio.1823.
31. Davies TG, Hubbard RE, Tame JR. 1999. Relating structure to thermodynamics: the crystal structures and binding affinity of eight OppA-peptide complexes. Protein Sci 8:1432–1444. https://doi.org/10.1110/ps.8.7.1432.
32. Sleigh SH, Seavers PR, Wilkinson AJ, Ladbury JE, Tame JR. 1999. Crystallographic and calorimetric analysis of peptide binding to OppA protein. J Mol Biol 291:393–415. https://doi.org/10.1006/jmbi.1999.2929.
33. Viguera E, Canceill D, Ehrlich S. 2001. Replication slippage involves DNA polymerase pausing and dissociation. EMBO J 20:2587–2595. https://doi.org/10.1093/emboj/20.10.2587.
34. Tizei PAG, Harris E, Renders M, Pinheiro VB. 2017. InDel assembly: a novel framework for engineering protein loops through length and compositional variation. bioRxiv https://doi.org/10.1101/127829.
35. Martínez-García E, de Lorenzo V. 2011. Engineering multiple genomic deletions in Gram-negative bacteria: analysis of the multi-resistant antibiotic profile of *Pseudomonas putida* KT2440. Environ Microbiol 13:2702–2716. https://doi.org/10.1111/j.1462-2920.2011.02538.x.
36. Martínez-García E, de Lorenzo V. 2012. Transposon-based and plasmid-based genetic tools for editing genomes of Gram-negative bacteria. Methods Mol Biol 813:267–283. https://doi.org/10.1007/978-1-61779-412-4_16.
37. Baba T, Ara T, Hasegawa M, Takai Y, Okumura Y, Baba M, Datsenko KA, Tomita M, Wanner BL, Mori H. 2006. Construction of *Escherichia coli* K-12 in-frame, single-gene knockout mutants: the Keio collection. Mol Syst Biol 2:2006.0008. https://doi.org/10.1038/msb4100050.
38. Thomason LC, Costantino N, Court DL. 2007. *E. coli* genome manipulation by P1 transduction. Curr Protoc Mol Biol Chapter 1:Unit 1.17. https://doi.org/10.1002/0471142727.mb0117s79.
39. Hanahan D. 1983. Studies on transformation of *Escherichia coli* with plasmids. J Mol Biol 166:557–580. https://doi.org/10.1016/S0022-2836(83)80284-8.
40. Sambrook J. 2001. Molecular cloning: a laboratory manual, 3rd ed. Cold Spring Harbor Laboratory Press, Cold Spring Harbor, NY.
41. Van Dyke MW, Sirito M, Sawadogo M. 1992. Single-step purification of bacterially expressed polypeptides containing an oligo-histidine domain. Gene 111:99–104. https://doi.org/10.1016/0378-1119(92)90608-R.
42. Gasteiger E, Gattiker A, Hoogland C, Ivanyi I, Appel RD, Bairoch A. 2003. ExPASy: the proteomics server for in-depth protein knowledge and analysis. Nucleic Acids Res 31:3784–3788. https://doi.org/10.1093/nar/gkg563.
43. Laemmli UK. 1970. Cleavage of structural proteins during the assembly of the head of bacteriophage T4. Nature 227:680–685. https://doi.org/10.1038/227680a0.
44. Langmead B, Salzberg SL. 2012. Fast gapped-read alignment with Bowtie 2. Nat Methods 9:357–359. https://doi.org/10.1038/nmeth.1923.
45. Langmead B, Trapnell C, Pop M, Salzberg SL. 2009. Ultrafast and memory-efficient alignment of short DNA sequences to the human genome. Genome Biol 10:R25. https://doi.org/10.1186/gb-2009-10-3-r25.
46. Gerstung M, Beisel C, Rechsteiner M, Wild P, Schraml P, Moch H, Beerenwinkel N. 2012. Reliable detection of subclonal single-nucleotide

variants in tumour cell populations. Nat Commun 3:811. https://doi.org/10.1038/ncomms1814.
47. Gerstung M, Papaemmanuil E, Campbell PJ. 2014. Subclonal variant calling with multiple samples and prior knowledge. Bioinformatics 30:1198–1204. https://doi.org/10.1093/bioinformatics/btt750.
48. Robinson JT, Thorvaldsdóttir H, Winckler W, Guttman M, Lander ES, Getz G, Mesirov JP. 2011. Integrative Genomics Viewer. Nat Biotechnol 29:24–26. https://doi.org/10.1038/nbt.1754.
49. Thorvaldsdóttir H, Robinson JT, Mesirov JP. 2013. Integrative Genomics Viewer (IGV): high-performance genomics data visualization and exploration. Brief Bioinformatics 14:178–192. https://doi.org/10.1093/bib/bbs017.
50. Platt R, Drescher C, Park SK, Phillips GJ. 2000. Genetic system for reversible integration of DNA constructs and *lacZ* gene fusions into the *Escherichia coli* chromosome. Plasmid 43:12–23. https://doi.org/10.1006/plas.1999.1433.
51. Messing J, Crea R, Seeburg PH. 1981. A system for shotgun DNA sequencing. Nucleic Acids Res 9:309–321. https://doi.org/10.1093/nar/9.2.309.
52. Yanisch-Perron C, Vieira J, Messing J. 1985. Improved M13 phage cloning vectors and host strains: nucleotide sequences of the M13mp18 and pUC19 vectors. Gene 33:103–119. https://doi.org/10.1016/0378-1119(85)90120-9.
53. Studier FW, Moffatt BA. 1986. Use of bacteriophage T7 RNA polymerase to direct selective high-level expression of cloned genes. J Mol Biol 189:113–130. https://doi.org/10.1016/0022-2836(86)90385-2.
54. Dykxhoorn DM, St. Pierre R, Linn T. 1996. A set of compatible *tac* promoter expression vectors. Gene 177:133–136. https://doi.org/10.1016/0378-1119(96)00289-2.
55. Martínez-García E, Aparicio T, Goni-Moreno A, Fraile S, de Lorenzo V. 2015. SEVA 2.0: an update of the Standard European Vector Architecture for de-/re-construction of bacterial functionalities. Nucleic Acids Res 43:D1183–D1189. https://doi.org/10.1093/nar/gku1114.
56. Bosshart A, Hee CS, Bechtold M, Schirmer T, Panke S. 2015. Directed divergent evolution of a thermostable D-tagatose epimerase towards improved activity for two hexose substrates. Chembiochem 16:592–601. https://doi.org/10.1002/cbic.201402620.
57. Billerbeck S, Panke S. 2012. A genetic replacement system for selection-based engineering of essential proteins. Microb Cell Fact 11:110. https://doi.org/10.1186/1475-2859-11-110.